

Differential effects of structural modifications on the competition of chalcones for the PIB amyloid imaging ligand-binding site in Alzheimer's disease brain and synthetic A β fibrils

Marina Y. Fosso , Katie L. McCarty, Elizabeth Head, Sylvie Garneau-Tsodikova, and Harry Levine, III

ACS Chem. Neurosci., **Just Accepted Manuscript** • DOI: 10.1021/acschemneuro.5b00266 • Publication Date (Web): 18 Dec 2015Downloaded from <http://pubs.acs.org> on December 21, 2015**Just Accepted**

“Just Accepted” manuscripts have been peer-reviewed and accepted for publication. They are posted online prior to technical editing, formatting for publication and author proofing. The American Chemical Society provides “Just Accepted” as a free service to the research community to expedite the dissemination of scientific material as soon as possible after acceptance. “Just Accepted” manuscripts appear in full in PDF format accompanied by an HTML abstract. “Just Accepted” manuscripts have been fully peer reviewed, but should not be considered the official version of record. They are accessible to all readers and citable by the Digital Object Identifier (DOI®). “Just Accepted” is an optional service offered to authors. Therefore, the “Just Accepted” Web site may not include all articles that will be published in the journal. After a manuscript is technically edited and formatted, it will be removed from the “Just Accepted” Web site and published as an ASAP article. Note that technical editing may introduce minor changes to the manuscript text and/or graphics which could affect content, and all legal disclaimers and ethical guidelines that apply to the journal pertain. ACS cannot be held responsible for errors or consequences arising from the use of information contained in these “Just Accepted” manuscripts.



1
2
3
4
5
6
7 Differential effects of structural modifications on the
8
9
10
11 competition of chalcones for the PIB amyloid
12
13
14
15
16 imaging ligand-binding site in Alzheimer's disease
17
18
19
20
21 brain and synthetic A β fibrils
22
23
24

25 *Marina Y. Fosso,^a Katie McCarty,^b Elizabeth Head,^{b,c} Sylvie Garneau-Tsodikova,^{a,*} Harry*
26 *LeVine, III^{c,d,e,*}*
27
28
29
30

31 ^a Department of Pharmaceutical Sciences, College of Pharmacy, University of Kentucky, 789
32 South Limestone Street, Lexington, KY, 40536-0596, USA. ^b Department of Pharmacology and
33 Nutritional Sciences, ^c Center on Aging, ^d Molecular and Cellular Biochemistry, and ^e Center for
34 Structural Biology, School of Medicine, University of Kentucky, Lexington, KY, 40536-0230,
35
36
37
38
39
40
41 USA.
42
43
44
45
46

47 **KEYWORDS** Displacement assay, Neurodegenerative disorder, Pittsburgh Compound B,
48
49
50 Radioactive assay, Structure activity relationships.
51
52
53
54
55
56
57
58
59
60

ABSTRACT

Alzheimer's disease (AD) is a complex brain disorder that still remains ill defined. In order to understand the significance of binding of different clinical *in vivo* imaging ligands to the polymorphic pathological features of AD brain, the molecular characteristics of the ligand interacting with its specific binding site need to be defined. Herein, we observed that tritiated Pittsburgh Compound B (^3H -PIB) can be displaced from synthetic $\text{A}\beta(1-40)$ and $\text{A}\beta(1-42)$ fibrils and from the PIB binding complex purified from human AD brain (ADPBC) by molecules containing a chalcone structural scaffold. We evaluated how substitution on the chalcone scaffold alters its ability to displace ^3H -PIB from the synthetic fibrils and ADPBC. By comparing unsubstituted core chalcone scaffolds along with the effects of bromine and methyl substitution at various positions, we found that attaching a hydroxyl group on the ring adjacent to the carbonyl group (ring I) of the parent member of the chalcone family generally improved the binding affinity of chalcones toward ADPBC and synthetic fibrils F_{40} and F_{42} . Furthermore, any substitution on ring I at the *ortho*-position of the carbonyl group greatly decreases the binding affinity of the chalcones, potentially as a result of steric hindrance. Together with the finding that neither our chalcones nor PIB interact with the Congo Red/X-34 binding site, these molecules provide new tools to selectively probe the PIB binding site that is found in human AD brain, but not in brains of AD pathology animal models. Our chalcone derivatives also provide important information on the effects of fibril polymorphism on ligand binding.

INTRODUCTION

In 2004 the benzothiazole aniline A β amyloid fibril ligand Pittsburgh Compound B (PIB) labeled with ^{11}C for positron emission tomography (PET) imaging was shown in a small study of living patients to be retained in brain areas known to accumulate A β pathology in Alzheimer's disease (AD) brains, but not in normal brains.¹ Subsequent studies showed that PIB uptake tracked with disease progression starting decades before cognitive symptoms were evident.^{2, 3} As the most widely clinically used A β deposition tracer, PIB is generally considered a benchmark for amyloid PET imaging agents.

The effort to find agents for early diagnosis of AD by imaging A β pathology in living patients has produced a variety of small molecule and peptide ligands (reviewed in ⁴). While many such molecules have been identified, little is known about which features of A β pathology are being reported and which ligands are recognizing the same feature or binding to the same site. Lockhart and colleagues defined distinct sites for ligands on synthetic A β fibrils based on their ability to compete for binding.^{5, 6} Other studies elaborated and confirmed the concept of multiple distinct sites on A β fibrils for ligands to bind.^{7, 8}

The significance of this multiplicity of ligand-binding sites was brought into sharp focus by the initial observation by Klunk and co-workers that the benzothiazole aniline ligand PIB bound with high affinity in large amounts to AD brain, but only very little bound to similar amounts of A β pathology in a transgenic mouse model of AD.⁹ High affinity ^3H -PIB binding was also negligible in other genetic and natural nonhuman primate and canine animal models of AD A β pathology.¹⁰ By contrast, ligands such as Congo Red and X-34 (Scheme 1D), which do not

1
2
3 compete for PIB binding and, therefore, bind to a site distinct from where PIB binds to A β
4
5 pathology, bound normally in these animal models. Since humans are the only animal that
6
7 suffers the full progression of AD, these findings suggested that the site to which PIB binds was
8
9 unique and that elucidation of how it was formed and its structure might provide insight into the
10
11 disease process and potential therapeutic avenues. Our determination that PIB binding A β
12
13 pathology was an isolatable fraction of the total AD brain A β pathology with different physical
14
15 properties and protein composition¹¹ indicated that high affinity PIB binding addressed a
16
17 reasonably discrete population of peptide conformers present at high levels in human AD brain
18
19 and only low levels in animal models.
20
21
22
23
24
25

26
27 These observations suggest that imaging ligands that bind to A β pathology at sites distinct
28
29 from the PIB binding site have the potential to be reporting different processes or to miss events,
30
31 both of which would foster confusion potentially leading to misinterpretation in diagnosis and in
32
33 defining progression mechanisms. Ni and colleagues showed in AD tissue homogenates that the
34
35 two ¹⁸F-labeled stilbene derivatives florbetapir (Amyvid™) and florbetaben (Neuraceq™)
36
37 (Scheme 1D) now used in the clinic, compete for PIB binding to AD brain tissue, as does
38
39 Vizamyli™ (flutemetamol; 2-[3-[¹⁸F]fluoro-4-(methylamino) phenyl]-6-benzothiazolol), a PIB
40
41 derivative.¹² Thus, imaging in AD brain with these ligands should give similar results to those
42
43 with ¹¹C-PIB.
44
45
46
47
48

49
50 PIB competition results have not been reported for the majority of ligands shown in
51
52 preclinical studies to bind A β pathology. Based on the fact that the chalcone scaffold (1,3-
53
54 diphenyl-2-propen-1-one, **DPP**, Scheme 1D) highly resembles the florbetaben and florbetapir
55
56 core, with the exception of the additional carbonyl group in **DPP**, and also based on the fact that
57
58
59
60

1
2
3 the *N,N*-dimethylamino/*N*-monomethylamino moieties of various molecules have been
4
5 demonstrated to be critical to A β , we hypothesized that chalcone derivatives containing an *N,N*-
6
7 dimethylamino group could potentially compete for the PIB binding site in A β . Here, we
8
9 demonstrate that molecules based on the chalcone scaffold displace ³H-PIB from the
10
11 Alzheimer's disease PIB binding complex (ADPBC) purified from AD brain, as well as from
12
13 more widely available model fibrils assembled from synthetic A β (1-40) and A β (1-42) peptides.
14
15 We also show that a prototypical chalcone of our series, **9a**, stains A β plaque pathology
16
17 selectively, and like PIB, does not stain tau pathology in tissue sections from hippocampus of
18
19 AD brain. Several series of electron-withdrawing, electron-donating, and bulky substituents on
20
21 ring I produced molecules with EC₅₀ values displaying consistent structure-activity relationships
22
23 (SAR). ³H-X-34 binding was unaffected by these chalcones (EC₅₀ values > 10 μ M).
24
25 Quantification of ³H-PIB binding to synthetic peptide A β (1-40) and A β (1-42) fibrils (indicated
26
27 from here on as F₄₀ and F₄₂, respectively) indicated a high A β :PIB stoichiometry, many A β s per
28
29 high affinity PIB binding site, while the purified ADPBC from AD brain showed nearly a 1:1
30
31 stoichiometry.¹⁰
32
33
34
35
36
37
38
39
40

41 We report that the SAR of chalcones for synthetic F₄₀ and F₄₂ fibrils differs from that of the
42
43 AD brain site, and that the F₄₀ and F₄₂ fibrils have SARs distinct from one another. This suggests
44
45 that the details of the binding site for chalcones that compete for PIB binding differ among the
46
47 different fibril populations.
48
49

50 51 **RESULTS AND DISCUSSION**

52 53 54 55 **Chemistry**

56
57
58
59
60

1
2
3
4
5
6
7
8
9
10
11
12
13
14
15
16
17
18
19
20
21
22
23
24
25
26
27
28
29
30
31
32
33
34
35
36
37
38
39
40
41
42
43
44
45
46
47
48
49
50
51
52
53
54
55
56
57
58
59
60

Chalcones have long been known as a prolific class of compounds, displaying a vast array of biological activities.¹⁴ With the aim of investigating their effects on the formation and dissociation of A β oligomers, we recently reported on the synthesis of three series of chalcones,¹⁵ differing from each other by the nature of ring I (Scheme 1C). They either bear a pyridine (compounds **3a-i**), a phenol (compounds **6a-h**), or an aniline (compounds **7a, b, h**) moiety as ring I. Electron-withdrawing, electron-donating, and bulky substituents, such as a methyl or a bromo group, were also introduced at various positions on ring I. We further expanded this series of chalcones by including compounds **8i** (Scheme 1A) and **9a** (Scheme 1B), which were obtained in 62 and 86% yields, respectively, by reacting 4-(dimethylamino)benzaldehyde, **2**, with the corresponding ketone (**1i** and **4a**, respectively) in the presence of a base (KOH or NaOH). Overall, the modifications on ring I were selected with the goals of (i) mimicking the pyridine ring of florbetapir and (ii) attaching handles that we could later potentially use to further derivatize our molecules and generate radiolabeled or fluorescently labeled compounds as imaging agents.

Investigation of unsubstituted core scaffolds

After establishing that our chalcones did not compete for binding with ³H-X-34 (all EC₅₀ values against ³H-X-34 > 10 μ M), we investigated the binding of the unsubstituted core scaffolds (**DPP**, **3a**, **6a**, **7a**, and **9a**) to ADPBC. The parent member of the chalcone family, **DPP** (Scheme 1D), was first evaluated and it was found to have better affinity for displacing ³H-PIB from ADPBC than synthetic F₄₀ and F₄₂ fibrils (Table 1, entry 23). While not as potent as the best benzothiazole aniline ligands (PIB: EC₅₀ = 2.6 nM; BTA-1: EC₅₀ = 3 nM),¹¹ it was sub-micromolar despite

1
2
3 missing the *N,N*-dimethylamino/*N*-monomethylamino moiety on the aromatic ring critical for the
4
5 benzothiazole aniline ligands.¹⁶
6
7

8 9 **Selectivity of chalcone scaffold for AD brain A β plaque pathology.**

10
11
12 Sections of hippocampal tissue from AD brain containing both A β plaque pathology and tau
13
14 neurofibrillary tangle pathology were stained with chalcone **9a** to verify its selectivity for the A β
15
16 pathology (Figure 1). Thioflavin S stains both A β plaques (white triangles) and tau pathology
17
18 (white arrows) in panel **A**. By contrast, like PIB and its analogue 6-CN-PIB, the chalcone stains
19
20 only the A β plaque pathology (white triangles) in an adjacent tissue section shown in panel **B**.
21
22 This selectivity convinced us of the potential ability of chalcones to effectively displace PIB
23
24 from its binding site in AD brain and in synthetic peptide model systems, and led us to
25
26 investigate the effects of substitution on the structural scaffold of **DPP**. The ratios of EC₅₀ values
27
28 shown in Table 1 for displacement of ³H-PIB from the different A β fibril sources also provide
29
30 insight into the relative similarity of the ligand-binding site on those fibrils. Large or small ratios
31
32 indicate that the compound binds differently to each type of fibrils, whereas ratios close to 1
33
34 indicate compounds with comparable affinity to the types of fibrils compared.
35
36
37
38
39
40
41
42

43
44 Upon attachment of a *N,N*-dimethylamino moiety on ring II and replacement of the benzene
45
46 ring I in **DPP** by a pyridine (**3a**, entry 1), phenol (**6a**, entry 10), or aniline (**7a**, entry 18) moiety,
47
48 we observed that the core scaffold **6a** binds better than the core scaffold **3a**, which in turn binds
49
50 better than **DPP** to ADPBC, F₄₀, and F₄₂ fibrils. Furthermore, **6a** and **7a** have comparable binding
51
52 affinity toward F₄₀ and F₄₂ fibrils, but the core scaffold **7a** does not bind as well as **6a** and **3a** to
53
54 ADPBC. It thus appears that having a phenol as ring I provides the strongest competitor to ³H-
55
56 PIB in ADPBC, F₄₀, and F₄₂ fibrils, while the presence of the benzene ring alone imparted the
57
58
59
60

1
2
3 weakest displacement of ^3H -PIB in all cases. Furthermore, when the hydroxyl group on **6a** was
4 moved away from position 1 to 2, as in **9a** (Table 1, entry 22), the binding affinity and fibril
5 selectivity were altered. Compound **6a** was better than **9a** at binding synthetic F_{40} fibrils, while
6 the opposite was observed for synthetic F_{42} fibrils. Not surprisingly though, the EC_{50} values for
7 the two compounds were similar in ADPBC, which may reflect the additional components
8 (lipids, other proteins) in the ADPBC. As a result, we decided to pursue our structural
9 modifications on ring I of core scaffolds **3a**, **6a**, and **7a**.
10
11
12
13
14
15
16
17
18
19

20 21 **Direct comparison of methylated and brominated core scaffolds**

22
23
24 By adding a methyl or bromo group at positions 2-5 of ring I, we were able to compare chalcone
25 derivatives with the same substituent at the same position in that ring. In the presence of F_{40}
26 fibrils, the EC_{50} values of chalcone derivatives **6a-h** (Figure 2B) with the phenol ring (entries 10-
27 17) were the smallest (highest affinity), in comparison to **3a-h** (Figure 2A) with a pyridine
28 moiety (entries 1-8) and **7a, b, and h** with an aniline (entries 18-20). In the case of F_{42} fibrils, any
29 substitution at position 2 or 5 will still make the chalcone derivatives with the phenolic ring
30 (entries 11, 14, and 15) better (lower EC_{50} , higher affinity) than their corresponding analogues
31 with the pyridine (entries 2, 5, and 6). On the other hand, if a methyl group is at position 3 or 4,
32 the chalcone derivatives from the pyridine (scaffold **3**; entries 3-4) and phenol (scaffold **6**; entries
33 12-13) series have comparable affinities; meanwhile a bromo group at position 3 or 4 will make
34 the chalcone derivatives with a pyridine moiety (entries 7-8) better competitor than the ones with
35 the phenol (entries 16-17). It thus appears that the presence of a weak electron-withdrawing
36 group (EWG) at position 3 or 4 will switch which one is better in F_{42} fibrils. In the case of
37 ADPBC, substitution did not seem to have a large effect, since the chalcone derivatives with the
38 phenol moiety had higher affinity than their counterparts with a pyridine or an aniline moiety,
39
40
41
42
43
44
45
46
47
48
49
50
51
52
53
54
55
56
57
58
59
60

1
2
3 with the exception of **6d** (entry 13) and **6h** (entry 17), which had higher EC₅₀ values (lower
4 affinity) than their respective pyridine analogues **3d** (entry 4) and **3h** (entry 8). Overall, **6a-h**
5 with the phenol moiety had higher affinity for ADPBC, F₄₀, and F₄₂ fibrils (Table 1, entries 10-
6 17) than their counterparts with a pyridine (**3a-h**, entries 1-8) or an aniline moiety (**7a, b**, and **h**,
7 entries 18-20), which confirms our initial findings that having a phenol moiety as ring I
8 conferred higher affinity binding to ADPBC, F₄₀, and F₄₂ fibrils. It is important to note that,
9 although not in all cases, overall, the more lipophilic compounds (higher log P values in Table
10 S1) displayed higher binding affinity to Aβ.
11
12
13
14
15
16
17
18
19
20
21
22

23 **Comparison of the effect of bromine *versus* methyl substitution**

24
25
26
27 When comparing the methyl group *versus* the bromo group as substituents on ring I, it appears
28 that the chalcone derivatives with the bromo group display comparable or higher affinity than
29 their methyl counterparts towards ADPBC, F₄₀, and F₄₂ fibrils, with the exception of **6f** (entry
30 15), **6g** (entry 16), and **6h** (entry 17), which did not bind synthetic F₄₂ fibrils as well as their
31 methyl counterparts **6b** (entry 11), **6c** (entry 12), and **6d** (entry 13), respectively. This suggests
32 that a weak EWG such as a bromo group might enhance the binding affinity of the chalcones.
33
34
35
36
37
38
39
40
41

42 **Comparison of the effect of substitution pattern on core scaffolds**

43
44
45 Regarding the effect on binding affinity of various positions for substitution on ring I of all three
46 core scaffolds (**3**, **6**, and **7**), we noticed that for synthetic F₄₀ fibrils, position 3 was generally
47 preferred over position 2, which in turn was preferred to position 4. In the case of ADPBC and
48 F₄₂ fibrils, position 2 was generally preferred over position 3, which in turn was preferred to
49 position 4 for the chalcone derivatives with the phenol moiety. Overall, position 5 appears to be
50 the least favored in most cases, probably due to the steric hindrance that might be created. We
51
52
53
54
55
56
57
58
59
60

1
2
3 also observed that moving the nitrogen of the pyridine ring away from the carbonyl moiety of the
4 chalcone, as in compound **8i** (entry 21), is disfavored and series **8** was therefore not further
5 investigated.
6
7
8
9

10
11 Previous SAR with the benzothiazole aniline series^{11, 16} suggests a relatively sterically
12 restricted binding pocket with a parallel SAR for ADPBC, F₄₀, and F₄₂ fibrils. The more flexible
13 chalcone scaffold is relatively tolerant of substituents. Interestingly, the chalcone derivatives
14 investigated here markedly distinguish among the ADPBC, F₄₀, and F₄₂ fibrils. This behavior
15 could reflect a different binding mode for chalcones, which probes the structural organization of
16 the fibrils around while occluding a subsite that binds the benzothiazole aniline moiety.
17 Chalcones could be especially sensitive to A β fibril polymorphism around the PIB binding site,
18 which is distinct from the pan-amyloid fibril-binding site for Congo Red and X-34.
19
20
21
22
23
24
25
26
27
28
29
30

31 CONCLUSIONS

32
33
34
35 In summary, we found that the chalcone scaffold widely reported as A β imaging tracers⁴
36 competes for ³H-PIB binding, but not for ³H-X-34 binding to synthetic A β (1-40) and A β (1-42)
37 fibrils and to the PIB-binding fraction of A β isolated from AD brain. As hypothesized,
38 exploration of a series of ring I substitutions revealed a consistent pattern of differential effects
39 on competition for ³H-PIB binding that differentiated the two synthetic peptide fibrils from each
40 other as well as from the AD brain material. Overall, the pattern of the EC₅₀ values of chalcone
41 displacement of ³H-PIB from PIB binding fraction from AD brain most closely resembled that of
42 the synthetic A β (1-42) fibrils (Table 1). Since the chalcones studied did not interact with the
43 Congo Red/X-34 binding site, they provide tools to explore details of A β fibril structure around
44
45
46
47
48
49
50
51
52
53
54
55
56
57
58
59
60

1
2
3 the PIB binding pocket and effects of fibril polymorphism on ligand binding, which may explain
4
5 the low binding of PIB to the A β pathology of animal models.
6
7

8 9 **METHODS**

10
11
12 **Materials and instrumentation.** Human autopsy tissue for preparation of the ADPBC was
13
14 obtained from the University of Kentucky Center on Aging Brain Bank of the Alzheimer's
15
16 Disease Center in accordance with federal and institutional IRB guidelines with informed
17
18 consent, and samples were de-identified to ensure the anonymity of subjects. The study conforms
19
20 to The Code of Ethics of the World Medical Association. All chemicals were purchased from
21
22 Sigma Aldrich (St. Louis, MO) and used without further purification. Chemical reactions were
23
24 monitored by thin layer chromatography (TLC) using Merck, Silica gel 60 F₂₅₄ plates.
25
26 Visualization was achieved using UV light and KMnO₄ stain (1.5 g KMnO₄, 10 g K₂CO₃, 1.25
27
28 mL 10% NaOH, 200 mL H₂O). ¹H and ¹³C NMR spectra were recorded at 400 and 100 MHz,
29
30 respectively, on a Varian 400 MHz spectrometer, using the indicated solvents. Chemical shift (δ)
31
32 is given in parts per million (ppm). Coupling constants (*J*) are given in hertz (Hz), and
33
34 conventional abbreviations used for signal shape are as follows: s = singlet; d = doublet; t =
35
36 triplet; m = multiplet; dd = doublet of doublets; dt = doublet of triplets. Liquid chromatography-
37
38 mass spectrometry (LCMS) was carried out using an Agilent 1200 series Quaternary LC system
39
40 equipped with a diode array detector, and Eclipse XDB-C₁₈ column (250 mm x 4.6 mm, 5 μ m),
41
42 and an Agilent 6120 Quadrupole MSD mass spectrometer (Agilent Technologies, Santa Clara,
43
44 CA). LCMS M + H signals were consistent with the expected molecular weights for all of the
45
46 reported compounds.
47
48
49
50
51
52
53
54
55
56
57
58
59
60

1
2
3
4
5
6
7
8
9
10
11
12
13
14
15
16
17
18
19
20
21
22
23
24
25
26
27
28
29
30
31
32
33
34
35
36
37
38
39
40
41
42
43
44
45
46
47
48
49
50
51
52
53
54
55
56
57
58
59
60

Synthesis of chalcone ligands. The synthesis and structural characterization of chalcones **3a-i**, **6a-h**, and **7a, b, h** were performed as previously described.¹⁵

Synthesis of chalcone 8i. A solution of 3-acetyl-2-bromopyridine (**1i**) (201 mg, 1.0 mmol) and 4-(dimethylamino)benzaldehyde (**2**) (150 mg, 1.0 mmol) in EtOH (5 mL) was treated with 3 mL of a 20% aqueous KOH solution and allowed to stir at rt for 3 h. Upon completion of the reaction, H₂O (5 mL) was added and the solid residues that formed were filtered out, rinsed with H₂O and ice-cold EtOH, and recrystallized from CH₂Cl₂/hexanes to give compound **8i** (R_f 0.17 in Hexanes:EtOAc/3:1) as dark yellow needles (226 mg, 68% yield): ¹H NMR (400 MHz, CDCl₃) δ 8.46 (dd, *J*₁ = 4.8 Hz, *J*₂ = 2.0 Hz, 1H, aromatic), 7.70 (dd, *J*₁ = 7.2 Hz, *J*₂ = 2.0 Hz, 1H, aromatic), 7.46 (dt, *J*₁ = 9.2 Hz, *J*₂ = 2.0 Hz, 2H, aromatic), 7.36 (d, *J* = 15.6 Hz, 1H, HC=CH-Ph), 7.37 (dd, *J*₁ = 7.2 Hz, *J*₂ = 4.8 Hz, 1H, aromatic), 6.89 (d, *J* = 15.6 Hz, 1H, HC=CH-Ph), 6.69 (dt, *J*₁ = 9.2 Hz, *J*₂ = 2.0 Hz, 2H, aromatic), 3.05 (s, 6H, N(CH₃)₂); ¹³C NMR (100 MHz, CDCl₃) δ 192.7, 152.5, 150.6, 148.8, 138.9, 138.7, 137.4, 130.9 (2 carbons), 122.5, 121.6, 120.4, 111.8 (2 carbons), 40.1 (2 carbons); *m/z* calcd for C₁₆H₁₅BrN₂O 330.0; found 331.0 [M+H]⁺.

Synthesis of chalcone 9a. The known compound **9a** was prepared as previously described.¹⁹ A solution of 3'-hydroxy acetophenone (**4a**) (68 mg, 0.5 mmol) and 4-(dimethylamino)benzaldehyde (**2**) (75 mg, 0.5 mmol) in EtOH (1.5 mL) was treated with NaOH pellets (400 mg, 10.0 mmol). The reaction was stirred at rt overnight until completion. Most of the solvent was then removed and 1 N aqueous HCl was added. The precipitate was filtered to give the known compound **MFY-4-8** (R_f 0.26 in Hexanes:EtOAc/3:1) as an orange solid (110 mg, 82% yield): ¹H NMR (400 MHz, CDCl₃, which matches the lit.¹⁹) δ 7.78 (d, *J* = 15.6 Hz, 1H, HC=CH-Ph), 7.56-7.50 (m, 4H, aromatic), 7.35 (t, *J* = 8.0 Hz, 1H, aromatic), 7.29 (d, *J* = 15.6

1
2
3 Hz, 1H, HC=CH-Ph), 7.03 (dd, $J_1 = 8.0$ Hz, $J_2 = 2.0$ Hz, 1H, aromatic), 6.69 (d, $J = 9.2$ Hz, 2H,
4 aromatic), 5.30 (s, 1H, OH), 3.04 (s, 6H, N(CH₃)₂).

5
6
7
8
9 **Preparation of A β fibrils.** AD brain ADPBC was purified from autopsy human AD frontal
10 cortex as previously described¹¹ and was stored in aliquots at -75 °C. For the recombinant A β
11 (rPeptide, Bogart, GA) 1 mg each of A β (1-40) (cat. A-1153-2, lot #6050840H) and A β (1-42)
12 (cat. A-1163-2, lot #4230842H) obtained as films dried from HFIP were dissolved in 900 μ L of
13 ice-cold distilled H₂O and kept on ice for 30 min with intermittent vortexing. 100 μ L of 10x PBS
14 (final concentration 20 mM sodium phosphate, 145 mM NaCl, pH 7.4) were added with
15 vortexing followed by 20 μ L of 2% w/v NaN₃. The solutions were transferred to separate screw
16 cap polypropylene tubes, sealed, and incubated at 37 °C for one week, vortexing briefly once
17 each day. Fibril formation was assessed by sedimentable Thioflavin T fluorescence.^{13,17} Aliquots
18 of fibrils (1 mg/mL) were frozen at -20 °C and thawed immediately before use.

19 20 21 22 23 24 25 26 27 28 29 30 31 32 33 34 35 **Radioligand binding assays:**

36
37
38 **³H-PIB binding.** ³H-PIB binding was assessed in A β preparations from AD brain and in fibrils
39 prepared from A β (1-40) and A β (1-42) recombinant peptides (F₄₀ and F₄₂, respectively).¹¹ For
40 binding studies 20 μ L of PBS containing purified ADPBC equivalent to 133.3 μ g wet weight of
41 original tissue, 100 ng F₄₀, or 50 ng F₄₂ were added to each of duplicate wells of a 96-well
42 polypropylene plate (Costar 3365). Under the conditions of the assay these quantities of A β gave
43 similar total amounts of ³H-PIB binding, 10-15% of the input radioactivity. 200 μ L of 1.2 nM
44 ³H-PIB (cat. VT 278 specific radioactivity = 70.2 Ci/mmol, Vitrax (Placentia, CA)) containing a
45 dose response of nonradioactive competitor at a final concentration of DMSO of 1% v/v in PBS
46
47
48
49
50
51
52
53
54
55
56
57
58
59
60

1
2
3 + 5% v/v EtOH was added to each well. Samples were incubated for 3 h at room temperature
4
5 without shaking, transferred to a 96-well Millipore Multiscreen HTS Hi Flow FB (GF/B) filter
6
7 plate, and filtered on a multi-well plate vacuum manifold (Millipore Corporation, Bedford, MA).
8
9 The filters were rapidly washed three times with 200 μ L of PBS + 5% v/v EtOH, dried, removed
10
11 from the plate, and placed in scintillation vials. 2 mL of BudgetSolve scintillation fluid were
12
13 added, and the vials capped and shaken before counting for ^3H in a Packard TriCarb 2500 TR
14
15 scintillation counter. Specific binding was calculated as (mean CPM of the two filters from wells
16
17 containing radioactive PIB + competitors) minus (CPM value from wells containing radioactive
18
19 PIB + 1 μ M nonradioactive BTA-1 competitor). EC_{50} values were determined by titrating
20
21 increasing concentrations of unlabeled test compound against constant (1.3 nM) ^3H -PIB. The
22
23 EC_{50} is the concentration at which 50% of the specifically bound ^3H -PIB is displaced. Although
24
25 the EC_{50} values are slightly greater than the IC_{50} values because more than 10% of the total
26
27 radioligand is bound, the EC_{50} values can be compared with each other since they were
28
29 determined under the same conditions.
30
31
32
33
34
35

36
37
38 **^3H -X-34 binding.** ^3H -X-34 binding¹⁸ was performed similarly to PIB binding with 5 nM ^3H -X-
39
40 34, 23 Ci/mmol, custom tritiated by Vitrox (Placentia, CA)) with 10 μ M X-34 or Congo Red as
41
42 nonradioactive X-34 competitor.
43
44

45
46 **Chalcone and thioflavin S histochemistry.** Formalin-fixed hippocampal sections from an AD
47
48 case (77 year old female, Braak VI, post mortem interval 4.15 h, ApoE 4/4), 8 μ m thick were
49
50 deparaffinized and rehydrated through decreasing concentrations of alcohol until washing in
51
52 PBS. Sections were incubated in a room temperature humidifier with 2 mM chalcone **9a** in 20%
53
54 v/v DMSO in PBS for 1 h in the dark. After 3x1 min PBS washes, sections were treated with
55
56
57
58
59
60

1
2
3 TrueBlack Lipofuscin Autofluorescence Quencher (30s-Biotium, Hayward, CA) and then
4 coverslipped using Everbrite Hardset Mounting Medium (Biotium, Hayward, CA). An adjacent
5 section was stained with thioflavin S (0.5% w/v in 50% v/v EtOH) for 5 min, then washed in 50%
6 EtOH, followed by ddH₂O, and then coverslipped using Vectashield with DAPI (Vector
7 Laboratories, Burlingame, CA). Images were captured using an Olympus BX51 fluorescence
8 microscope with a wide band pass filter.
9
10
11
12
13
14
15
16
17

18 ASSOCIATED CONTENT

21
22 **Supporting Information.** The supporting information includes a copy of the ¹H and/or ¹³C NMR
23 spectra for compounds **8i** and **9a**. It also includes a table containing the log P values for all of our
24 compounds (Table S1). This material is available free of charge *via* the Internet at
25 <http://pubs.acs.org>.
26
27
28
29
30
31
32
33

34 AUTHOR INFORMATION

36 Corresponding Authors

37
38
39
40 * Harry LeVine, III: E-mail: hlevine@email.uky.edu
41
42

43 or

44
45 Sylvie Garneau-Tsodikova: E-mail: sylviegttsodikova@uky.edu
46
47
48
49
50

51 Funding Sources

52
53 This work was supported by startup funds from the University of Kentucky (to S.G.-T.) and by
54 NIH grant AI90048 (to S.G.-T.), and by NIH grant 1R21 NS080576-01A1 (to H.L.), and NIH
55
56
57
58
59
60

1
2
3 Center Core grant P30AG028383 (Alzheimer's Disease Center). The content is solely the
4 responsibility of the authors and does not necessarily represent the official views of the National
5 Institutes of Health. The authors declare no competing financial interest.
6
7
8
9

10 11 12 13 **ACKNOWLEDGMENTS**

14
15 This work was supported by startup funds from the University of Kentucky (to S.G.-T.) and by
16 NIH grant AI90048 (to S.G.-T.) and by NIH grant 1R21 NS080576-01A1 (to H.L.), and NIH
17 Center Core grant P30AG028383 (Alzheimer's Disease Center). We thank Dr. David S. Watt for
18 initial compounds implicating chalcones as PIB-displacing A β ligands. We acknowledge Linda
19 Van Eldik, Ph.D. Sanders-Brown Director, Peter Nelson, M.D., Ph.D., Neuropathology Core
20 Director, and Sonya Anderson, Brain Bank Coordinator for human brain tissue and their
21 contributions on behalf of the ADC. We are forever in debt to the patients whose brain donations
22 made this investigation possible.
23
24
25
26
27
28
29
30
31
32
33

34 35 **REFERENCES**

- 36
37
38 1. Klunk, W. E., Engler, H., Nordberg, A., Wang, Y., Blomqvist, G., Holt, D. P., Bergstrom,
39 M., Savitcheva, I., Huang, G. F., Estrada, S., Ausen, B., Debnath, M. L., Barletta, J., Price, J.
40 C., Sandell, J., Lopresti, B. J., Wall, A., Koivisto, P., Antoni, G., Mathis, C. A., and
41 Langstrom, B. (2004) Imaging brain amyloid in Alzheimer's disease with Pittsburgh
42 Compound-B. *Ann. Neurol.* 55, 306-319.
43
44
45
46
47
48
49 2. Jack, C. R., Jr., Knopman, D. S., Jagust, W. J., Petersen, R. C., Weiner, M. W., Aisen, P. S.,
50 Shaw, L. M., Vemuri, P., Wiste, H. J., Weigand, S. D., Lesnick, T. G., Pankratz, V. S.,
51 Donohue, M. C., and Trojanowski, J. Q. (2013) Tracking pathophysiological processes in
52
53
54
55
56
57
58
59
60

- 1
2
3 Alzheimer's disease: an updated hypothetical model of dynamic biomarkers. *Lancet Neurol.*
4
5
6 12, 207-216.
7
- 8 3. Jack, C. R., Jr., Barrio, J. R., and Kepe, V. (2013) Cerebral amyloid PET imaging in
9
10 Alzheimer's disease. *Acta Neuropathol.* 126, 643-657.
11
- 12 4. Eckroat, T. J., Mayhoub, A. S., and Garneau-Tsodikova, S. (2013) Amyloid-beta probes:
13
14 Review of structure-activity and brain-kinetics relationships. *Beilstein J. Org. Chem.* 9, 1012-
15
16 1044.
17
- 18 5. Lockhart, A., Ye, L., Judd, D. B., Merritt, A. T., Lowe, P. N., Morgenstern, J. L., Hong, G.,
19
20 Gee, A. D., and Brown, J. (2005) Evidence for the presence of three distinct binding sites for
21
22 the thioflavin T class of Alzheimer's disease PET imaging agents on beta-amyloid peptide
23
24 fibrils. *J. Biol. Chem.* 280, 7677-7684.
25
26
27
28
- 29 6. Ye, L., Morgenstern, J. L., Gee, A. D., Hong, G., Brown, J., and Lockhart, A. (2005)
30
31 Delineation of positron emission tomography imaging agent binding sites on beta-amyloid
32
33 peptide fibrils. *J. Biol. Chem.* 280, 23599-23604.
34
35
- 36 7. Lockhart, A. (2006) Imaging Alzheimer's disease pathology: one target, many ligands. *Drug*
37
38 *Discov. Today* 11, 1093-1099.
39
- 40 8. LeVine, H., 3rd. (2005) Multiple ligand binding sites on A beta(1-40) fibrils. *Amyloid* 12, 5-
41
42 14.
43
44
- 45 9. Klunk, W. E., Lopresti, B. J., Ikonovic, M. D., Lefterov, I. M., Koldamova, R. P.,
46
47 Abrahamson, E. E., Debnath, M. L., Holt, D. P., Huang, G. F., Shao, L., DeKosky, S. T.,
48
49 Price, J. C., and Mathis, C. A. (2005) Binding of the positron emission tomography tracer
50
51 Pittsburgh compound-B reflects the amount of amyloid-beta in Alzheimer's disease brain but
52
53 not in transgenic mouse brain. *J. Neurosci.* 25, 10598-10606.
54
55
56
57
58
59
60

- 1
2
3
4
5
6
7
8
9
10
11
12
13
14
15
16
17
18
19
20
21
22
23
24
25
26
27
28
29
30
31
32
33
34
35
36
37
38
39
40
41
42
43
44
45
46
47
48
49
50
51
52
53
54
55
56
57
58
59
60
10. Rosen, R. F., Walker, L. C., and Levine, H., 3rd. (2011) PIB binding in aged primate brain: enrichment of high-affinity sites in humans with Alzheimer's disease. *Neurobiol. Aging* 32, 223-234.
 11. Matveev, S. V., Spielmann, H. P., Metts, B. M., Chen, J., Onono, F., Zhu, H., Scheff, S. W., Walker, L. C., and LeVine, H., 3rd. (2014) A distinct subfraction of Abeta is responsible for the high-affinity Pittsburgh compound B-binding site in Alzheimer's disease brain. *J. Neurochem.* 131, 356-368.
 12. Ni, R., Gillberg, P. G., Bergfors, A., Marutle, A., and Nordberg, A. (2013) Amyloid tracers detect multiple binding sites in Alzheimer's disease brain tissue. *Brain* 136, 2217-2227.
 13. LeVine, H., 3rd. (1993) Thioflavin T interaction with synthetic Alzheimer's disease beta-amyloid peptides: detection of amyloid aggregation in solution. *Protein Sci.* 2, 404-410.
 14. Batovska, D. I., and Todorova, I. T. (2010) Trends in utilization of the pharmacological potential of chalcones. *Curr. Clin. Pharmacol.* 5, 1-29.
 15. Fosso, M. Y., LeVine 3rd, H., Green, K. D., Tsodikov, O. V., and Garneau-Tsodikova, S. (2015) Effects of structural modifications on the metal binding, anti-amyloid activity, and cholinesterase inhibitory activity of chalcones. *Org. Biomol. Chem.* 13, 9418-9426.
 16. Klunk, W. E., Wang, Y., Huang, G. F., Debnath, M. L., Holt, D. P., Shao, L., Hamilton, R. L., Ikonovic, M. D., DeKosky, S. T., and Mathis, C. A. (2003) The binding of 2-(4'-methylaminophenyl)benzothiazole to postmortem brain homogenates is dominated by the amyloid component. *J. Neurosci.* 23, 2086-2092.
 17. LeVine, H., 3rd. (1999) Quantification of beta-sheet amyloid fibril structures with thioflavin T. *Methods Enzymol.* 309, 274-284.

- 1
2
3 18. Matveev, S. V., Kwiatkowski, S., Sviripa, V. M., Fazio, R. C., Watt, D. S., and LeVine, H.,
4
5 3rd. (2014) Tritium-labeled (*E,E*)-2,5-bis(4'-hydroxy-3'-carboxystyryl)benzene as a probe for
6
7 beta-amyloid fibrils. *Bioorg. Med. Chem. Lett.* 24, 5534-5536.
8
9
10 19. Zhao, P. L., Liu, C. L., Huang, W., Wang, Y. Z., and Yang, G. F. (2007) Synthesis and
11
12 fungicidal evaluation of novel chalcone-based strobilurin analogues. *J. Agric. Food Chem.*
13
14 55, 5697-700.
15
16
17
18
19
20
21
22
23
24
25
26
27
28
29
30
31
32
33
34
35
36
37
38
39
40
41
42
43
44
45
46
47
48
49
50
51
52
53
54
55
56
57
58
59
60

SCHEME LEGEND

Scheme 1. Synthetic scheme for the preparation of **A.** chalcone **8i** and **B.** chalcone **9a**. **C.** Structures of chalcones **3a-i**, **6a-h**, and **7a, b, h**. **D.** Structures of DPP, PIB, BTA-1, X-34, florbetaben (^{18}F), and florbetabir (^{18}F).

FIGURE LEGENDS

Figure 1. Thioflavin S and chalcone **9a** labeling in the hippocampus of an AD case. **A.** Thioflavin S binds to plaques (white triangles) and neurofibrillary tangles (white arrows) in area CA1 of the hippocampus. **B.** In contrast, chalcone **9a** binds to plaques (white triangles), but not neurofibrillary tangles in an adjacent section from the same case. Scale bar = 40 μm .

Figure 2. Displacement of ^3H -PIB from ADPBC by **A.** chalcones **3a-i** and **B.** chalcones **6a-h**. Percent maximal ^3H -PIB binding = (binding in absence of competitor – binding in presence of 1 μM BTA-1). Mean of two assays on separate days \pm SDEV.

TABLE LEGENDS

Table 1. EC_{50} values (μM) of chalcone competition for ^3H -PIB binding to $\text{A}\beta$ preparations.

Scheme 1.

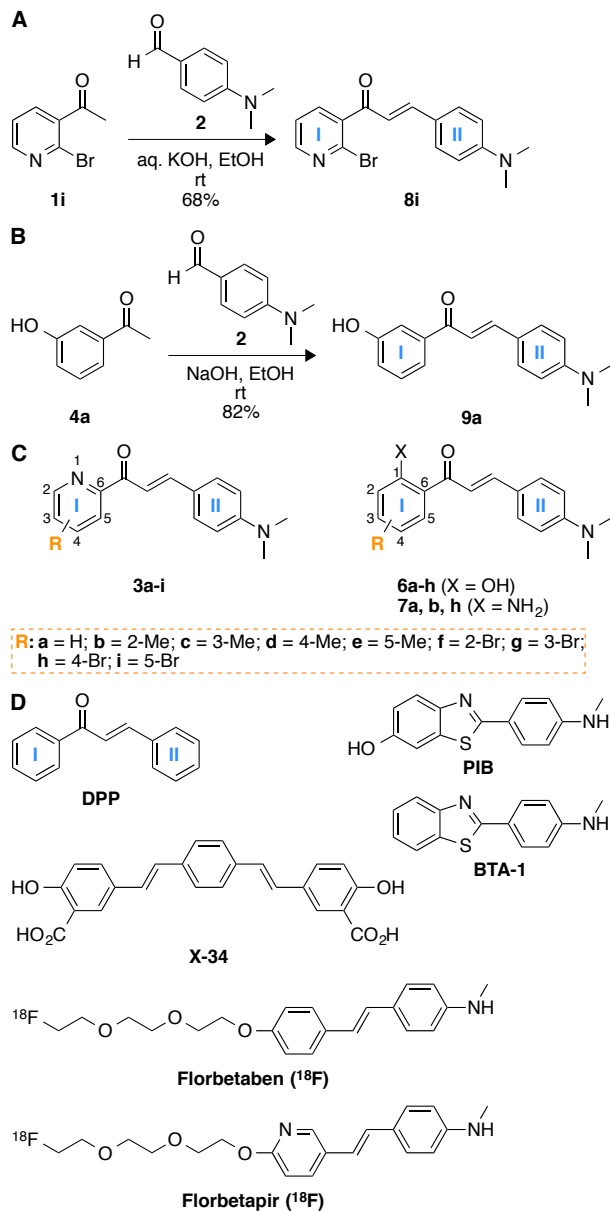


Figure 1.

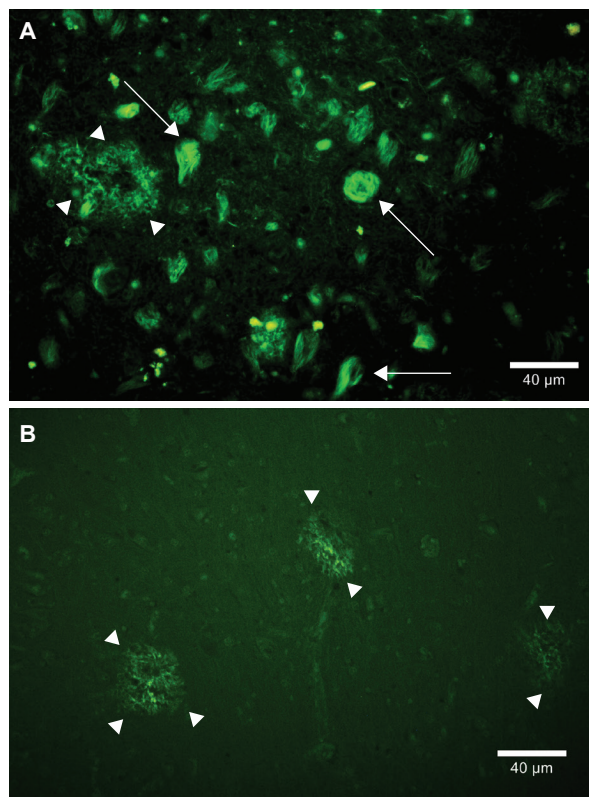


Figure 2.

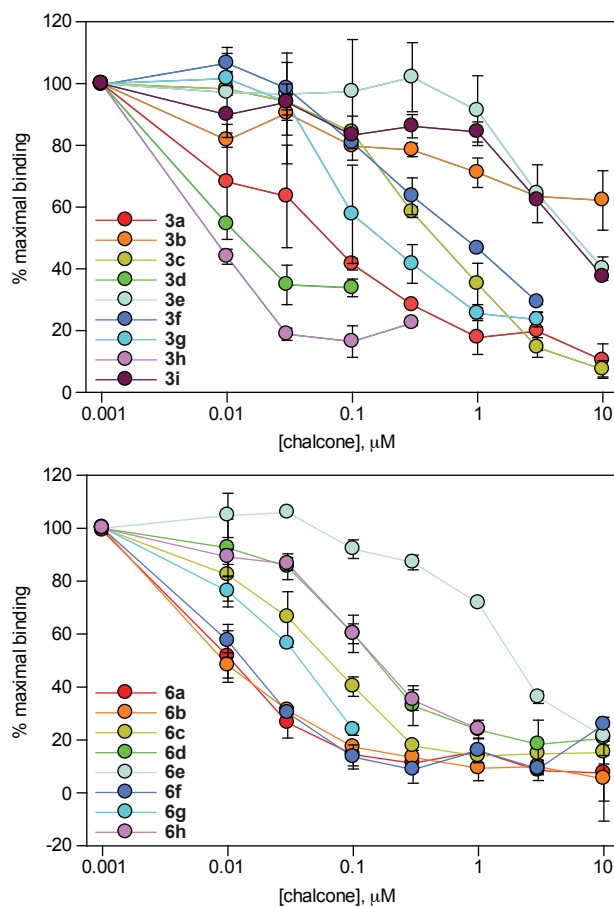


Table 1. EC₅₀ values (μM) of chalcone competition for ³H-PIB binding to Aβ preparations^a.

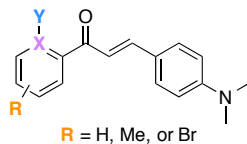
Entry	Cpd #	F ₄₀	F ₄₂	ADPBC	Ratio of EC ₅₀ values ^b		
					F ₄₀ /F ₄₂	F ₄₀ /ADPBC	F ₄₂ /ADPBC
1	3a	1.150 ± 0.071	0.350 ± 0.057	0.037 ± 0.005	3.3	31	9.5
2	3b	4.200 ± 0.283	1.850 ± 0.636	> 10	2.3	^c	^c
3	3c	2.100 ± 0.707	0.097 ± 0.005	0.465 ± 0.078	22	4.5	0.2
4	3d	> 10	0.125 ± 0.007	0.013 ± 0.001	^c	^c	10
5	3e	5.100 ± 1.556	3.700 ± 0.707	6.050 ± 1.344	1.4	0.8	0.6
6	3f	1.150 ± 0.071	0.555 ± 0.021	0.795 ± 0.035	2.1	1.4	0.7
7	3g	0.765 ± 0.049	0.105 ± 0.007	0.142 ± 0.069	7.3	5.4	0.7
8	3h	0.515 ± 0.120	0.026 ± 0.006	0.008 ± 0.001	20	64	3.3
9	3i	9.000 ± 1.414	4.300 ± 1.414	8.000 ± 1.414	2.1	1.1	0.5
10	6a	0.030 ± 0.004	0.120 ± 0.028	0.010 ± 0.003	0.3	3	12
11	6b	0.083 ± 0.014	0.063 ± 0.010	0.009 ± 0.003	1.3	9.2	7.0
12	6c	0.058 ± 0.001	0.110 ± 0.014	0.056 ± 0.021	0.5	1.0	2.0
13	6d	0.570 ± 0.339	0.170 ± 0.042	0.185 ± 0.035	3.4	3.1	0.9
14	6e	2.250 ± 0.212	1.800 ± 0.849	1.650 ± 0.071	1.3	1.4	1.1
15	6f	0.150 ± 0.014	0.125 ± 0.007	0.014 ± 0.004	1.2	11	8.9
16	6g	0.050 ± 0.000	0.410 ± 0.014	0.032 ± 0.001	0.1	1.6	13
17	6h	0.220 ± 0.014	0.520 ± 0.028	0.150 ± 0.042	0.4	1.5	3.5
18	7a	0.035 ± 0.006	0.110 ± 0.014	0.059 ± 0.002	0.3	0.6	1.9
19	7b	0.270 ± 0.085	0.082 ± 0.040	0.010 ± 0.002	3.3	27	8.2
20	7h	1.050 ± 0.071	0.675 ± 0.078	> 10	1.6	^c	^c
21	8i	> 10	9.000 ± 1.414	> 10	^c	^c	^c
22	9a	0.165 ± 0.064	0.036 ± 0.008	0.013 ± 0.001	4.6	13	2.8
23	DPP	9.500 ± 0.707	1.750 ± 0.495	0.650 ± 0.071	5.4	15	2.7
24	PIB	0.015 ± 0.007	0.040 ± 0.005	0.003 ± 0.001	0.4	4.3	11.6
25	BTA-1	0.026 ± 0.007	0.031 ± 0.002	0.003 ± 0.001	0.8	8.8	10.5

^a F₄₀ = Aβ(1-40) fibrils; F₄₂ = Aβ(1-42) fibrils; ADPBC = PIB binding site isolated from AD brain (see Methods).

^b Large or small ratios indicate that the compound binds differently to each fibril type, whereas ratios close to 1 indicate compounds with comparable affinity to the fibril types compared.

^c Due to solubility-micellarization concerns which interfere with ³H-PIB binding measurements, compounds were not tested at concentrations greater than 10 μM and no ratio can be calculated in this case.

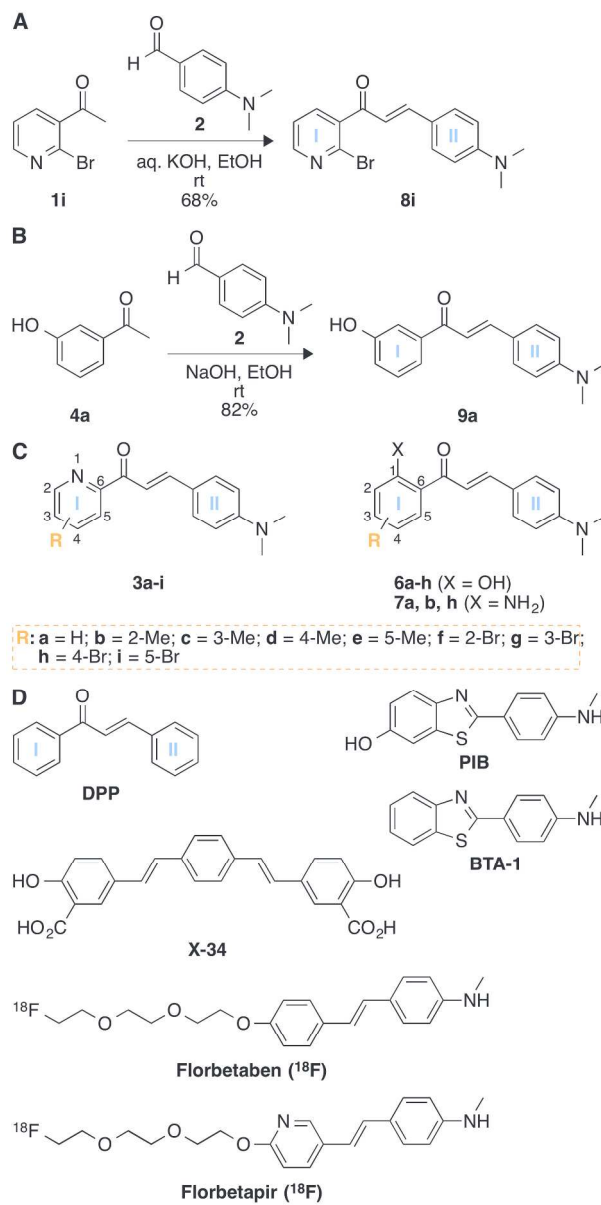
1
2
3 **Table of Contents Graphic and Synopsis.**
4
5



12 **³H-PIB displacement:**

13 (X = C; Y = OH) > (X = C; Y = NH₂) > (X = N) > (X = C; Y = H)

14
15
16 **Novel molecules compete for PIB binding to A β :** Our synthesized chalcones are very specific
17
18 to the PIB binding site, with the phenolic moiety imparting the greatest affinity.
19
20
21
22
23
24
25
26
27
28
29
30
31
32
33
34
35
36
37
38
39
40
41
42
43
44
45
46
47
48
49
50
51
52
53
54
55
56
57
58
59
60



Scheme 1.tif
160x317mm (300 x 300 DPI)

1
2
3
4
5
6
7
8
9
10
11
12
13
14
15
16
17
18
19
20
21
22
23
24
25
26
27
28
29
30
31
32
33
34
35
36
37
38
39
40
41
42
43
44
45
46
47
48
49
50
51
52
53
54
55
56
57
58
59
60

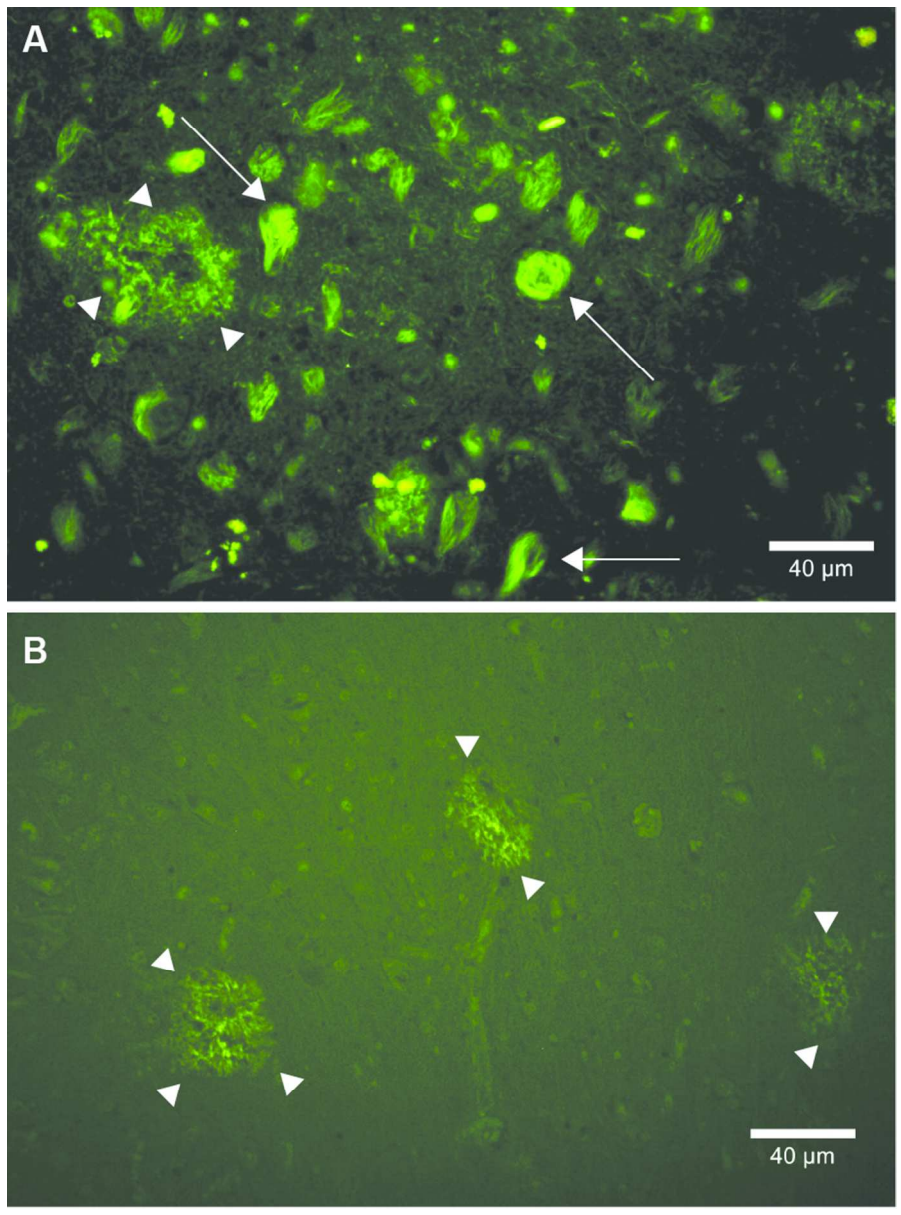


Figure 1.tif
77x104mm (300 x 300 DPI)

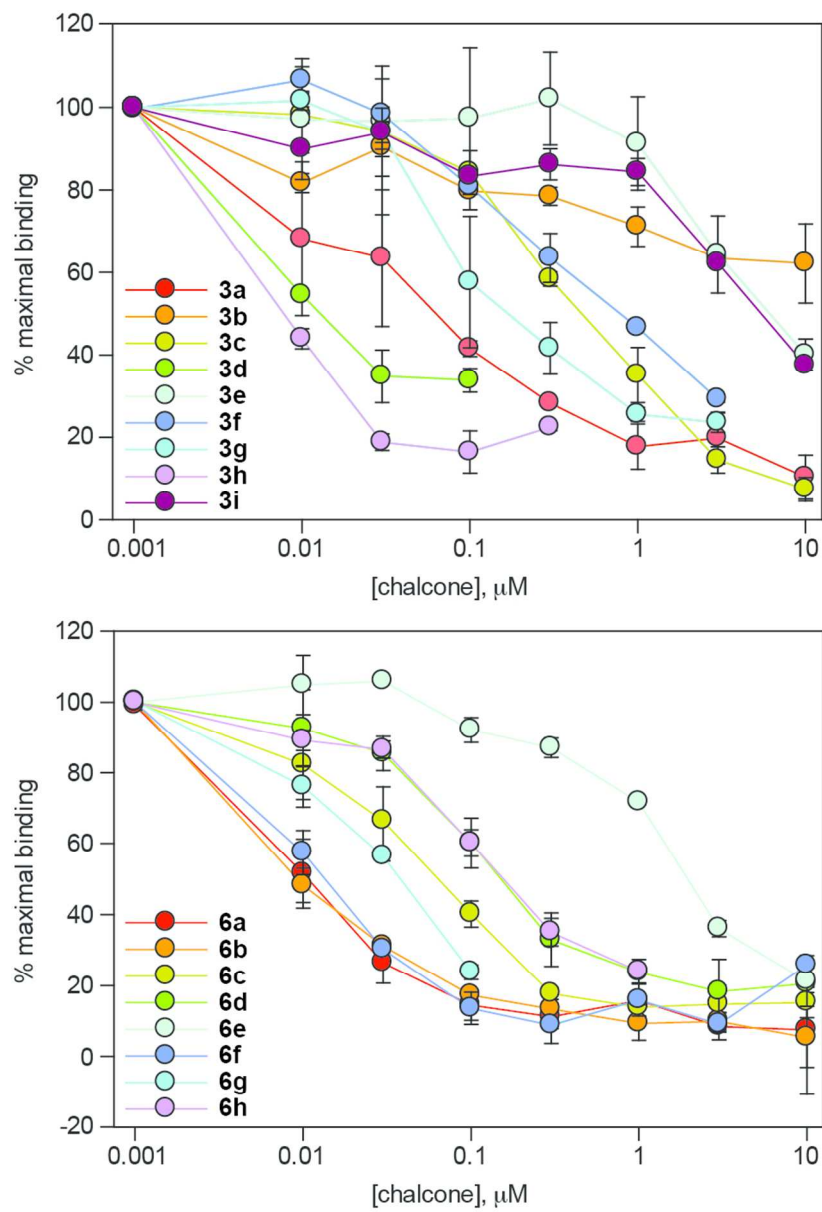
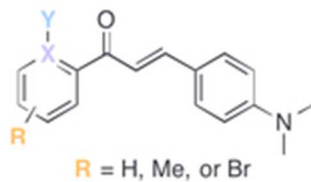


Figure 2.tif
80x118mm (300 x 300 DPI)



³H-PIB displacement:

$(X = \text{C}; Y = \text{OH}) > (X = \text{C}; Y = \text{NH}_2) > (X = \text{N}) > (X = \text{C}; Y = \text{H})$

Image for Table of content.tif
28x11mm (300 x 300 DPI)